

In vitro amino acid and glucose uptake rates across the gut wall of a surface deposit feeder

Robert F.L. Self^{a,*}, Peter A. Jumars^a, Lawrence M. Mayer^b

^a*School of Oceanography, University of Washington, Box 357940, Seattle, WA 98195-7940, USA*

^b*Department of Oceanography, University of Maine, Walpole, ME 04573, USA*

Received 2 August 1994; revision received 27 March 1995; accepted 20 April 1995

Abstract

We used the everted-sleeve method (Karasov & Diamond, 1983) and dual radiolabelled substrates to measure carrier-mediated and diffusive fluxes of glucose and four amino acids (AA) across the gut wall of the mobile, surface deposit-feeding holothuroid *Parastichopus californicus* Stimpson. The relationship between substrate concentration and carrier-mediated uptake rate for D-glucose, L-aspartic acid, L-glutamic acid, L-methionine, and L-tyrosine was adequately described by the classic Michaelis-Menten equation. Passive uptake rates were controlled by substrate interaction with the hydrophobic gut membrane. For the hydrophilic compounds (glucose, methionine and aspartic and glutamic acids) passive uptake contributed 11% or less to total uptake but accounted for 21% of the total for the rare but hydrophobic AA L-tyrosine.

Carrier-mediated uptake rates of hydrophilic (and lipophobic) AA were inversely proportional to the relative availability of substrate in sedimentary food. Balance in absorptive delivery was achieved by compensating for rarity in sedimentary food (low luminal concentration) and retarded cross-membrane diffusion with added carriers. Thus the relatively rare (in the food) and lipophobic AA L-methionine possessed the highest carrier-mediated maximal flux ($J_{max} = 57 \text{ pM (mg wet mass of gut tissue)}^{-1} \text{ min}^{-1}$) as well as the highest apparent half-saturation concentration. Glucose, aspartic and glutamic acid, all relatively common sediment organic constituents with intermediate passive permeabilities, had intermediate J_{max} values ranging from 6 to 26 $\text{pM} \cdot \text{mg}^{-1} \cdot \text{min}^{-1}$. The rare but lipophilic and thus highly permeant AA L-tyrosine had the lowest J_{max} of 2.6 $\text{pM} \cdot \text{mg}^{-1} \cdot \text{min}^{-1}$, with passive diffusion accounting for substantial uptake.

The distribution of nutrient uptake rates along the gut depends upon substrate carrier densities and luminal concentrations of the products of digestion. Rates interpolated at regional (fore-, mid- and hindgut) concentrations were high in the foregut and midgut but decreased in the hindgut for the rare AA methionine and tyrosine; conversely they were

* Corresponding author.

low in the foregut and high in both midgut and hindgut for the common AA glutamic and aspartic acid. Despite these varying patterns of AA flux along the gut, when integrated over the whole gut length to estimate total amount of AA absorbed, just as in the sediment food and animal tissue the acidic AA dominated while tyrosine was rare. The total amount of methionine absorbed far surpassed tissue requirements, however, suggesting that it is hyperessential. Our results indicate that AA compositional equality of uptake ratios with food and tissue composition ratios serves as a useful null hypothesis for identifying hyperessential nutrients. Karasov has used AA: sugar uptake ratios to classify vertebrates as herbivores, omnivores or carnivores. By this criterion *Parastichopus californicus* is clearly a herbivore, showing a very low ratio.

Keywords: Deposit feeder; Digestion; Gut; Holothuroid; Hyperessential nutrient; Nutrient absorption

1. Introduction

A long-standing question in the study of deposit feeders (Lopez et al., 1989) is the source of their nutrition. Bulk characterization of sediments by total organic content and coarse subdivision into nitrogen and carbon moieties have given some clues. It has been found, for example, that some shallow-water deposit feeders do not obtain the bulk of their carbon from the living bacterial component (Cammen, 1989). Difficulties in narrowing the possibilities for major food resources arise from the prodigious rates of feeding—a median of 3.7 times their own body mass of sediments per day (Cammen, 1980), with rates of some species on dilute foods up to 100× higher (Taghon, 1988). These rates allow even a minor sedimentary constituent, if extracted with modest to high efficiency, to contribute substantially to nutrition (Cammen, 1989). What is less obvious is that such high feeding rates virtually assure ingestion of “unwanted” food particles; rejection becomes more difficult and presumably more costly at high ingestion rates (Jumars, 1993). In short, analyzing what goes in is not a reliable means for narrowing the range of possible answers to the question of food source. Because patch selection for food quality and mechanical selection prior to ingestion do usually occur and because at the high throughput rates of food only a small fraction must be assimilated, attempting to estimate uptake from input-output (ingested material versus defecated remains) analysis has inherently low precision. Its accuracy also is highly suspect unless selection is assessed accurately.

For a few deposit feeders or detritivores manipulations of food supplies in the laboratory and the field have produced less equivocal evidence regarding sources of nutrition. Prinslow et al. (1974) showed with detrital supplements to the diet that detritus played no major role in nutrition of the primarily carnivorous killifish (*Fundulus heteroclitus*). Manifold approaches (e.g. Robertson & Newell, 1982; Wolfrath, 1992) paint a convincing picture of members of the fiddler crab genus *Uca* as patch specialists on benthic diatoms. Perhaps the most convincing combination of field and laboratory studies points toward digestive and absorptive

specialization by members of the snail genus *Hydrobia* on benthic diatoms (e.g. Fenchel & Kofoed, 1976; Bianchi & Levinton, 1984). Microphytobenthos is implicated as the dominant food source for other common intertidal deposit feeders as well (e.g. Hummel, 1985; Stuart et al., 1985). Manipulative methods become strikingly more difficult for subtidal organisms, however, and the inference of dominance by microphytobenthos clearly cannot be extended below the intertidal without evidence.

For these reasons, and because of the guidance offered by optimal digestion and absorption theory (Penry & Jumars, 1987; Dade et al., 1990), we elected as a complementary approach to focus on processing of food inside the animal, specifically on digestion of proteins and absorption of the products. We chose to measure amino acids because proteins are strongly implicated in growth-rate limitation of at least some deposit feeders (Newell, 1965; Tenore et al., 1984; Taghon & Greene, 1990). This focus on internal events has some advantages. Rapid gut throughput becomes an ally, because only those chemical species that can be released from sediments and absorbed quickly need to be considered (Mayer et al., 1995). The clear disadvantage is the rarity of *in vivo* or *in vitro* information on either digestion or absorption in deposit feeders. Moreover, to test Dade et al.'s (1990) hypothesis that throughput rate is set to maximize the net rate of absorption requires, at a minimum, luminal concentrations of absorbed substrates, absorption rates as a function of those concentrations and throughput rates to be known. While this goal has been achieved for hummingbirds (Martinez del Rio & Karasov, 1990), whose digestive and absorptive substrates are well known, it is more remote for any deposit feeder. Invertebrate digestion (Ahearn, 1988) in general has received less attention than vertebrate (e.g. Karasov, 1988), and among invertebrate feeding guilds deposit feeders are perhaps the least studied. Because past studies in deposit-feeding polychaetes (Bamford & Stewart, 1973a,b), holothuroids (Lawrence et al., 1967; Farmanfarmaian, 1969a,b; Farmanfarmaian et al., 1982) and echinoids (Bamford et al., 1972; Bamford & James, 1972) used varying techniques, often with contradictory results (reviewed in Ahearn, 1988), it is even more difficult to generalize.

A point that needs some attention is the relevance of uptake studies using monomers. It has been established in bacteria (Payne, 1980), invertebrates (Stewart, 1981; Thamocharan & Ahearn, 1995) and vertebrates (Matthews, 1975; Gardner, 1984) that protein uptake can occur in the form of oligomers of up to about 5–7 units as well as in monomer form. Oligomer (versus monomer) uptake can constitute a substantial proportion of the total depending on protein source (Gardner, 1982). The current concept for vertebrates is that a significant quantity of peptide is transported into the gut cells, but that it is largely free AA (~70%) that enter the circulatory system (Alpers, 1987). The oligomer uptake system appears to be H^+ rather than Na^+ dependent, and some small peptides are hydrolysis resistant (e.g. Matthews & Adibi, 1976; Minami et al., 1992). If a particular amino acid limits growth rate, then the uptake response anticipated is proliferation of uptake sites for that amino acid both in monomer and oligomer form. It is difficult to predict the role of passive uptake for oligomers in

Parastichopus; while the diffusion coefficient would be decreased, the gradient driving diffusion could be increased by higher luminal concentrations as well as by hydrolysis to monomers at the external gut wall and (or) upon entry into gut cells, with subsequent passing of monomers into the haemal system.

In our preliminary exploration, direct assessment of oligomer uptake would be costly (price of custom-labelled oligomers) and premature, as the kinetics, energy sources and identities of hydrolysis-resistant oligomers are still being investigated (Plauth et al., 1992; Thwaites et al., 1993). Regardless of expense, the number of possible permutations of AA in even small oligomers is daunting in advance of a clear rationale for particular choices. Our choice of monomers, by contrast, was simple. We chose two abundant ones (aspartic and glutamic acids) and two rare ones (methionine and tyrosine) based on the analysis of food by Mayer et al. (1995, their Fig. 4).

Our limited goal in the present study was to assess the applicability of modern *in vitro* methods—devised for measuring absorption in vertebrates (Karasov & Diamond, 1983)—to the deposit-feeding problem. To progress most rapidly, we selected the largest deposit feeder easily available to us, i.e. the holothuroid *Parastichopus californicus* Stimpson. It has been studied enough to allow its digestive system to be classified roughly as a plug flow reactor (Penry, 1989). To develop and test methodology for direct measurement of absorption rate, we first used glucose, a molecule available in a variety of labeled forms. We found carrier-mediated uptake of Michaelis-Menten form for glucose as well as for all four AA.

2. Materials and methods

2.1. General procedures

Animals were collected subtidally near the Friday Harbor Laboratories, San Juan Island, Washington, USA. Individuals were kept in 0.3×0.6 m flowing-seawater water tables (10 to 14°C) at the Laboratories and allowed to feed *ad libitum* on sand from False Bay, San Juan Island, that had passed a 500- μ m sieve.

Only feeding individuals were used. Feeding rates were monitored by measuring gut throughput times of a trace amount of bacteria-coated (*Vibrio anguillarum*) fluorescent paint pigment powder (Radiant Color, Richmond, California). When placed in the animal's immediate feeding area, a portion of the tracer was quickly ingested, and we removed the remainder from the sediment surface. Gut throughput time in a plug-flow gut equals the time to the first sighting of a fecal pellet with a distinct band of unmixed tracer (Penry, 1989).

The animal's contracted size (Yingst, 1982) was measured before removing the gut either surgically or by inducing evisceration by injecting 10–15 ml of 1 molar KCl solution through the body wall into the coelomic cavity (Smith & Greenberg, 1973). Most of the animals to date ($n = 70$) have survived evisceration to regenerate the gut in 4–6 months. Obtaining the gut by either evisceration or

dissection causes aneurism, i.e. distension of thin-walled sections. The likely cause is the animals' response to any handling, which is to shut off fluid outflow through the anus while contracting the body wall around the coelomic fluid. The coelomic fluid is pressurized, forcing it through the walls of the gut. Recovery of eviscerated individuals is enhanced if KCl concentration in the coelomic cavity is reduced immediately, for example by forcing seawater through the mouth opening.

The removed gut was quickly transferred to filtered seawater and stored at 0°C. Observations and morphological measurements for each run included gut fullness, presence or absence of developing gonads and total gut length, as well as run starting and ending times.

2.2. Measurement of luminal concentrations

Samples for luminal concentrations of amino acids and glucose were obtained from separate individuals immediately upon removal of the gut. They were taken from the lumen by syringe without prefiltration. Any solids were removed by centrifugation before analysis.

Dissolved free amino acids in the gut fluid were analyzed after trichloroacetic acid (TCA) precipitation of larger peptides. The resultant supernatant was injected directly into a St. Johns Associates HPLC that uses ion exchange separation with post-column orthophthaldialdehyde (OPA) derivitization and fluorescence detection.

Dissolved glucose in the gut fluid was measured spectrophotometrically using an enzymatic approach, after deproteinization. Glucose was oxidized by glucose oxidase and the accompanying hydrogen peroxide measured by its oxidation of *o*-dianisidine to a colored form in the presence of added peroxidase. We used a commercially available kit and procedure (Sigma #510DA).

2.3. Tissue preparation and mounting

We followed Karasov & Diamond (1983); 1 cm long segments were cut by scalpel and sediment removed by gentle jets of cold seawater from a pasteur pipette. Under a dissecting microscope the section was then everted on a glass rod (hooked at one end like a shepherd's staff), exposing the luminal surface of the gut. The piece was then slipped onto a close-fitting glass rod 4–8 mm in diameter (chosen to fit the individual's gut diameter) by 20 cm long, retained in place with waxed dental floss at each end and the length measured through an ocular micrometer. The sleeve was rinsed again to remove any remaining, adherent sediment particles.

Elapsed time to measurement of the first sleeve was ≈ 10 min. Mounted sleeves were used immediately while unmounted tissue was kept in filtered seawater (changed regularly) at 0°C for up to 12 h. The prolonged storage time did not significantly affect carrier-mediated uptake rates (results not shown). All sleeves were run individually, with incubation times, gut section and substrate concentration randomized to avoid systematic errors.

2.4. Flux determinations

The ^{14}C -labelled probe molecules D-glucose, L-methionine, L-tyrosine, L-aspartic acid, L-glutamic acid and PEG (4000 MW polyethylene glycol) and the ^3H -labelled molecules L-glucose and PEG were obtained from New England Nuclear, Boston, MA. Incubation solutions were prepared with artificial seawater (Sigma Chemical), filtered seawater or holothurian Ringer's solution (Lawrence et al., 1967) and then dispensed in 8-ml aliquots to 140 × 16 mm diameter, flat-bottomed test tubes. Radiolabelled substrates were then added such that minimal tissue and solution counts were 100 × greater than background. An incubation bath sample was taken before incubating each tissue sample for determining probe and marker concentrations. Rod-mounted sleeves were pre-incubated for 5 min in oxygen-saturated (with an air bubbler), filtered seawater (kept at ambient seawater temperature of 10–14°C), then transferred to the incubation solutions (also kept at 10–14°C). During incubation the solution was agitated by stirring at 1200 rpm (checked by stroboscope) with a 10 × 3 mm stir-bar to restrict unstirred-layer effects. Because the sea cucumber gut is tightly packed with sediment and not a turbulent fluid environment, our measured fluxes are upper bounds. After up to 16 min the incubation was terminated by rinsing for 20 s (see Results) in 75 ml cold (0°C), filtered seawater (also stirred at 1200 rpm) or removed from the glass rod without rinsing, blotted to remove excess fluid, placed in tared glass scintillation vials and weighed. For dry mass, the segment was dried overnight at 55°C. Negligible loss of probe and marker from the bath coupled with no changes in bacterial counts (acridine orange stain method; Parsons et al., 1984) suggested that we could freeze and reuse incubation baths.

The samples were prepared for counting by adding 1–4 ml of tissue solubilizer (Soluene 350, Packard Instrument Co.) then cooked 24–48 h at 55°C. After cooling, 10 ml of scintillation cocktail (BCS, Amersham Corp.) was added. Finally, the solution was neutralized by addition of 60 μl of 100% acetic acid per milliliter of solubilizer.

Radioactivity was determined on a Beckman LS7800 liquid scintillation spectrometer using the H number technique of automatic external quench monitoring with nominal window settings as follows: ^3H -channel 0–400, ^{14}C -channel 400–670. The instrument has an automatic quench compensation feature that minimizes spill-over by varying window settings as a function of H number. Quench standards were prepared by adding 0–1.15 ml of solubilized tissue solution (pH 6.7) to 10 vials containing 10 ml scintillation cocktail and a known amount of radioactivity. The standards were counted, obtaining counting efficiency (for ^{14}C and ^3H) and quench number, through which a third-order polynomial calibration curve was fitted ($R^2 \geq 0.8$; $n \geq 73$). Counting efficiencies and ^{14}C -spill were (for ^3H -, ^{14}C - and ^{14}C -spill, respectively) 40, 74 and 18% in bathing solutions and 23, 68 and 18% in tissue samples. We followed Horrock's (1977) dual-label computations to convert from CPM to DPM. Typical 95% confidence limits for sample incubation bath concentrations were $\pm 6\%$, while the propagated errors for fluxes were $\pm 15\%$.

Isotope or other solute associated with a tissue sample is termed solute “space” (Karasov & Diamond, 1983). Nutritionally important solutes can be partitioned into three components, an extracellular part and two intracellular parts. The two intracellular parts result from diffusive and carrier-mediated transport across the cell membrane. Each component can be isolated and quantified by subtracting appropriately paired and labelled substrates. For example, PEG is a conservative marker in that it is not transported into intracellular spaces. It has no known carrier, and its molecular size prevents diffusion across the membrane. In mixtures with actively or passively transportable molecules, tracer PEG space measures the extracellular or adherent component. Solute spaces were calculated as Q/C , where Q = DPM associated with 1 cm of tissue, C = DPM of solute per μl of incubation solution, and “space” has units of $\mu\text{l} \cdot \text{cm}^{-1}$. The choice of the term is unfortunate, as the units and concept correspond to those of a partition coefficient.

Pairing D-glucose (known to have a carrier) with tracer L-glucose (which has identical permeability and adherent characteristics as D-glucose but no known carrier) and differencing quantifies carrier-mediated uptake of D-glucose. Pairing L-glucose and tracer PEG (which is impermeable and thus measures the adherent component) and differencing the amounts of each absorbed by the gut sleeve isolates the diffusive glucose component.

Amino acid (AA) kinetics are more difficult to quantify because L- and D-stereoisomers each can have carriers (Bamford & Stewart, 1973a,b). If concentrated AA ($200\text{--}2500 \times$ the half-saturation constant) and tracer PEG are paired, however, such that the AA carrier-mediated uptake system is immediately saturated, diffusive uptake dominates; subtracting PEG space corrects for the extracellular component, and a permeability coefficient that quantifies interaction with the lipid cell membrane can be determined (Stevens et al., 1982). We used a 2 mM concentration for L-tyrosine (solubility limit) and 20 mM for L-methionine, L-aspartic acid and L-glutamic acid. If adjacent sleeves of the same gut are used to also determine L-glucose permeability coefficients (also 20 mM concentration and paired with tracer PEG), then reliable AA: L-glucose permeability coefficient ratios can be determined. Incubation time was 6 min. Permeability coefficients were calculated as flux divided by concentration and have units of $\mu\text{l} \cdot \text{cm}^{-1} \cdot \text{min}^{-1}$ or $\mu\text{l} \cdot \text{mg}^{-1} \cdot \text{min}^{-1}$.

To estimate carrier-mediated AA uptake at dilute AA concentrations, we paired AA with tracer L-glucose. Justifications for this approach are that molecular weights are similar and that the alternative method of pairing AA with tracer PEG does not isolate the carrier-mediated component. Tissue AA space includes the extracellular, diffusive intracellular and carrier-mediated, intracellular components. L-glucose space (which includes the extracellular component) multiplied by the AA: L-glucose permeability coefficient ratio estimates the AA extracellular and diffusive intracellular components. Subtracting (AA extracellular + diffusive intracellular) from (AA extracellular + diffusive intracellular + carrier-mediated intracellular) yields the AA carrier-mediated, intracellular component.

We calculated probe uptake rates as

$$J = \frac{\left[\frac{R}{H_p} - \left(\frac{M}{H_m} \cdot \frac{C_p}{C_m} \cdot \frac{P_p}{P_m} \right) \right]}{t \cdot s}, \quad (1)$$

where R = probe DPM associated with the tissue sample, M = marker DPM of the tissue sample, H = DPM per nanomole, C = incubation solution concentration, P = permeability coefficient, t = incubation time, and s = tissue wet mass or length, while the subscripts p and m refer to the probe and marker, respectively. J has units of picomoles \cdot mg⁻¹ \cdot min⁻¹ or nanomoles \cdot cm⁻¹ \cdot min⁻¹ depending on the units of s .

2.5. Rinse and incubation times

Rinse-time experiments determined the time required to remove radioactive substrate physically attached to the surface of the gut sleeve. This material, if not removed, would lead to an overestimate of the amount of substrate taken into gut tissue. Protracted rinse times would cause substrate taken up during incubation to diffuse out of the cells, however, generating uptake underestimates. The best rinse time balances adequate removal of adhering substrate with limited substrate efflux from intracellular spaces (Karasov & Diamond, 1983).

Methods used to select the best post-incubation rinse time followed those for flux determinations except that two adjacent gut sleeves from foregut, midgut or hindgut were incubated for 8 min. Then one was rinsed for a randomly selected time (0, 10 and 20 s, 1, 3 and 5 min) while the other was processed without rinsing (zero rinse time). The relative effect of rinsing was expressed as percent substrate remaining: (rinsed tissue substrate concentration/unrinsed tissue substrate concentration) \times 100. This procedure allows comparison of rinse-time treatments across all gut sections.

Loosely bound substrate is removed quickly, as indicated by the initially steep slope of lines connecting median proportion of substrate remaining on tissue samples (Fig. 1). The substantial decrease in wash-off rate at rinse times greater than 1 min, coupled with the absence of further rate changes (Fig. 1) suggests that at greater rinse times intracellular substrate is refluxing out of the cells. Given these results, we used a 20-s rinse time in all subsequent experiments.

Incubation times should exceed the time required for bulk substrate to diffuse to and through the fluid layers immediately adjacent to the cell walls (unstirred or diffusive sublayer), set such that uptake is linear at high and low substrate concentrations and long enough to accumulate accurately measurable radioactivity (Karasov & Diamond, 1983). Tracer PEG solution was used to determine the time lag for solute concentration equilibration in the unstirred layer (adjacent to the cell surface) with the bulk incubation solution. The amount of PEG adhering to gut sleeves was measured for incubation times from 30 s to 10 min. PEG space reached half-maximum at 2 min and full equilibrium after 6 min of incubation

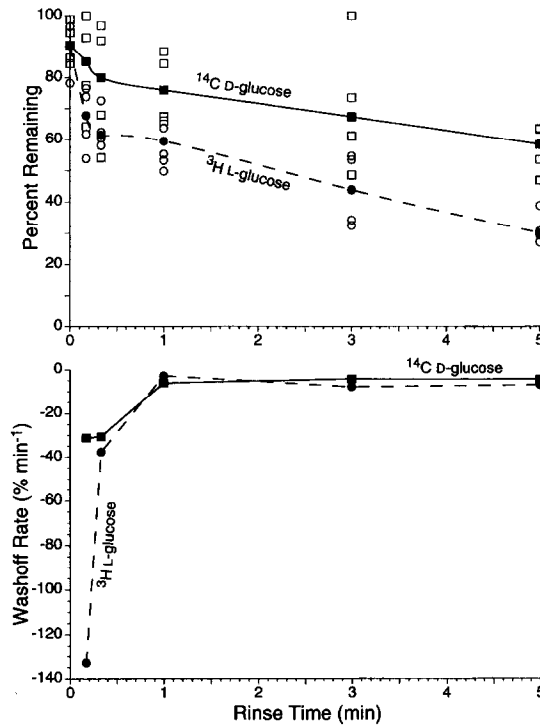


Fig. 1. Effect of rinse time on relative substrate concentration remaining and rate of wash-off from incubated *Parastichopus californicus* gut sleeves. Each rinse-time point represents the ratio of tissue substrate concentration (normalized to sleeve length) from two (rinsed-unrinsed) gut tissue samples incubated for 8 min in a dual-labelled (^{14}C D-glucose [\square] and ^3H L-glucose [\circ]) solution. Line connects median values (\blacksquare, \bullet). Sample size = 24. Note the difference in wash-off rate between L- and D-glucose. The D-isomer is removed more slowly because more of it is intracellular. L-glucose is removed faster because more of this substrate is physically attached. Between 20 s and 1 min rinse time the wash-off rate equilibrates. Extending the rinse time beyond 20 s increases the loss of intracellular material by diffusion.

(Fig. 2). Thus, if PEG were to be used to correct substrate uptake for adherent material, a minimal 6-min incubation time would be required for PEG in the bathing solution to diffuse and adhere to the cell membrane's surface. We assume for application to other molecules that the bulk of this equilibration behavior reflects diffusion into an unstirred layer of fluid at the lumen wall rather than surface chemical interaction of PEG with tissues.

An equilibration (and minimal incubation) time for L- and D-glucose space can be approximated from the PEG space results because the controlling process is diffusion, and molecular diffusion coefficients are inversely proportional to molecular weights. Extrapolating from the known diffusion coefficient for mannitol (MW 182.2) at 25°C of $6.8 \times 10^{-6} \cdot \text{cm}^2 \cdot \text{s}^{-1}$ (Weast, 1979), and applying a temperature correction to 10°C, $D_{10}/D_{25} = 0.65$ (Li & Gregory, 1974), we

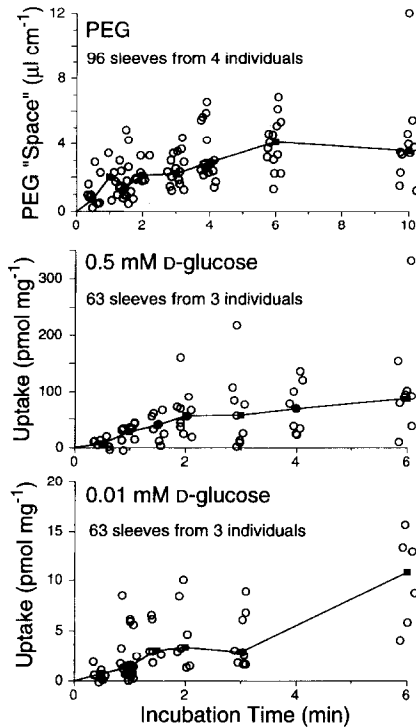


Fig. 2. Tissue uptake of PEG and D-glucose versus duration of gut sleeve incubation. D-glucose uptake is corrected for adherent substrate and diffusive uptake by subtracting the ^3H L-glucose uptake. \circ , individual sleeves; they are "jittered" (i.e. each moved slightly in a random direction) to reduce overlap (SYSTAT). \blacksquare , show the medians at the incubation times accurately (not jittered).

estimated substrate diffusion coefficients as $[182.2/(\text{MW})]^{1/3} \cdot 4.4 \times 10^{-6} \cdot \text{cm}^2 \cdot \text{s}^{-1}$ (Karasov & Diamond, 1983). Diffusion coefficients for PEG (MW 4000), glucose, tyrosine, methionine, aspartic acid and glutamic acid were calculated to be 1.6, 4.4, 4.4, 4.7, 4.9, and $4.7 \times 10^{-6} \cdot \text{cm}^2 \cdot \text{s}^{-1}$, respectively.

From the ratio of PEG:glucose diffusion coefficients we calculate the 1/2 saturation time for glucose to be 43 s with full equilibration at 2 min (Table 1). Thus 2 min would be a minimal incubation time for accurate assessment of glucose uptake by *Parastichopus* gut tissue. The amino acid substrates have molecular weights similar to glucose's and thus similar minimal incubation times (Table 1).

Maximal incubation time is generally controlled by bulk solute concentration. A high bathing solution substrate concentration means a steeper concentration gradient to the diffusive sublayer and thus rapid equilibration of an active uptake-dominated system. At high substrate concentrations within the unstirred layer carrier systems saturate sooner and uptake rates decline. These considerations set an upper bound on substrate concentration for exploration of con-

Table 1
Chemical and physiological characteristics of substrates

Substrate	Solubility in fresh water (mM) at 10°C ^a	Effect of salts on amino acid solubility ^b	Equilibration time (min) ^c	Incubation time (min) ^d
D-glucose	5045		2.1	2
L-aspartic acid	21	+	1.9	3
L-glutamic acid	34	+	2.0	2
L-methionine	293	–	2.0	4
L-tyrosine	2	–	2.1	3

^a Sober, 1970, Table B-66; Windholz, 1983, pp. 638–639.

^b McMeekin, 1975.

^c Based on experimentally determined 6-min equilibration time of PEG.

^d Experimentally determined except for tyrosine.

centration dependence of substrate flux across the gut wall (assuming that Michaelis-Menten kinetics apply). We would prefer to use ecologically relevant substrate concentrations reflecting those likely to be found in the guts of field-collected animals.

Farmanfarmaian (1969a) measured D-glucose concentrations of order 0.1 mM in *Thyone briareus* gut fluid. Our exploratory uptake measurements at 50 mM, then 1 mM D-glucose concentration clearly showed that the carrier-mediated transport system was immediately saturated, and the diffusive component dominated cross-membrane flux (Self & Jumars, unpubl.). These results coupled with measurable tissue uptake at micromolar D-glucose concentrations suggested 0.01–0.5 mM to be a workable concentration range for investigation of glucose uptake kinetics. Uptake rates (slopes of lines connecting medians) decline after a 2-min incubation in 0.5 mM D-glucose bathing solution (Fig. 2). At 0.01 mM, incubation times can be extended to 6 min without significant decrease in rates (Fig. 2). Apparently, at 0.5 mM the D-glucose carrier system begins to saturate as soon as full equilibration with the diffusive sublayer is reached.

Similar experiments with the amino acid substrates resulted in incubation times of 2–4 min (Table 1). We performed the uptake rate-vs.-concentration experiments using the tabled incubation times followed by 20-s rinses.

2.6. Statistical procedures

We utilized nonparametric linear (Tate & Clelland, 1957; Hollander & Wolfe, 1973) and nonlinear (Duggleby, 1981) regression in initial estimates of equation coefficients. Estimates were further refined such that the median residual was minimized and equal numbers of points lay above and below the line or curve (Tate & Clelland 1957). The nonlinear saturation model was accepted only if it improved significantly the fit between flux and concentration. We followed the model-fitting protocol of Box et al. (1978) to evaluate the nonparametric regressions. Deviations from model predictions were squared, then summed; mean squares and *F* ratios were calculated and compared to tabled values. The

nonlinear saturation model was accepted if it significantly ($p < 0.06$) increased the explained sum of squared deviations over the linear regression model. The large (and unequal) variance of the flux measurements suggested that medians, rather than means, were best for computation of experimental error. The probability levels of acceptance of the nonlinear model are conservative because residuals were squared, accentuating the contribution of outliers. Also, the linear models were not forced through zero, resulting in a better (lower sum of squared residuals) fit that increases this model's explained sum of squares. The greater the explained sum-of-squared deviations of the linear model, the less likely it is that the fit could be improved by the nonlinear Michaelis-Menten model.

The interpolation technique that we used retains the variability of the original flux measurements. The substrate flux (J) and incubation solution concentration were measured for each gut sleeve. From fitted regression parameters (see Table 2) expected fluxes could be calculated at the measured (J_m) and interpolated concentration (J_i). Estimated flux at the interpolated concentration (\hat{J}) is set up in the ratio

$$\frac{\hat{J}}{J_i} = \frac{J}{J_m} \quad (2)$$

and calculated. The disparity between J and J_m at the experimental concentration is retained at the interpolated concentration by a corresponding disparity between \hat{J} and J_i . Interpolated uptake rates were used to explore dependence on attributes of individual sleeves from different animals, such as storage time and gut location.

Some of the figures were drawn with the aid of SYSTAT for the Macintosh, Version 5.2 (Wilkinson et al., 1992). This use is indicated by parenthetical

Table 2
Results of flux versus concentration experiments. Median and nonparametric 95% confidence limits

Substrate	Passive permeability coefficient [95% CL] ($\mu\text{l} \cdot \text{mg}^{-1} \cdot \text{min}^{-1}$) $\times 10^{3b}$	J_{max} [95% CL] (pmol $\text{mg}^{-1} \cdot \text{min}^{-1}$) ^b	K_m [95% CL] (μM)	Contribution of diffusion to total uptake at K_m (%)
D-glucose	13 [9–17]	26 [20–37]	122 [63–135]	11
L-aspartic acid	17 [7–45]	6.7 [6–11]	13 [8–21]	6
L-glutamic acid	21 [0–30]	7.9 ^a [7–14]	8.3 ^a [7–10]	4 ^a
L-methionine	15 [9–23]	57 [41–74]	99 [72–110]	5
L-tyrosine	65 [13–135]	2.6 ^a [2–245]	5.3 ^a [5–16]	21 ^a

^a Mid- and hindgut fluxes only.

^b Per milligram tissue wet mass.

reference (SYSTAT). Some of these figures, in turn, use a more general interpolation procedure for smoothing scatterplots, i.e. LOWESS (Cleveland, 1979). We employ this procedure because it is relatively insensitive to outliers and makes no assumptions about the shape of the underlying curve. In all cases, we used the default value (Cleveland, 1979; SYSTAT parameter $F = 0.5$) for the extent of smoothing.

3. Results and discussion

3.1. Gut luminal morphology

Nominal gut diameter varied from 5–9 mm and gut lengths from 50–90 cm. We recognized four regions: esophagus (no uptake measurements made), fore-, mid- and hindgut. The three primary sections are of nearly equal length and correspond to Hyman's (1955) stomach-descending small intestine, ascending small intestine and large intestine, respectively. Demarcation points were based on luminal morphology, mass distribution, water content and externally-connected haemal sinus network.

Increased diameter denotes the beginning of the foregut. The most obvious internal features in longitudinal sections are the numerous ($\geq 80 \text{ cm}^{-1}$) lamellae intruding into the luminal space (Fig. 3A). Visible lamellar structures (Fig. 3B) give apparent fore-, mid- and hindgut surface areas of 8, 1, and $3 \text{ cm}^2 (\text{cm gut length})^{-1}$, respectively, for a nominal 0.5-cm gut diameter. A brown fluid always present in the anterior foregut displays potent hydrolytic and surfactant properties (Mayer et al., 1995 and unpubl. data). Secretory epithelial cells are prevalent, and in the posterior foregut sediments are always embedded in thick, mucous secretions. The foregut-midgut interface is marked externally by the beginning of the haemal sinus network and internally by diminished or absent lamellae. The midgut wall is thinner, internally smooth (Fig. 3C) and connected to the bulk of the haemal network. The midgut also shows high enzyme activity (Mayer et al., 1995). The end of the haemal network demarks the midgut-hindgut interface. The hindgut wall thickens posteriorly, and the initially smooth luminal wall becomes rugose (Fig. 3D). Here, enzyme activity is considerably reduced (Mayer et al., unpubl. data).

The distribution of mass per unit of length along the gut is roughly quadratic and correlates with surface area (Fig. 4). Increased hindgut mass is in part due to greater water content. For any given wet mass, dry tissue mass is least in the hindgut (Fig. 5).

3.2. Uptake rate versus concentration

L-glucose is the best diffusive marker for quantifying carrier-mediated uptake kinetics of D-glucose and AA, but its shortcomings should be realized even if they cannot be quantified. D- and L-glucose have identical molecular weights and

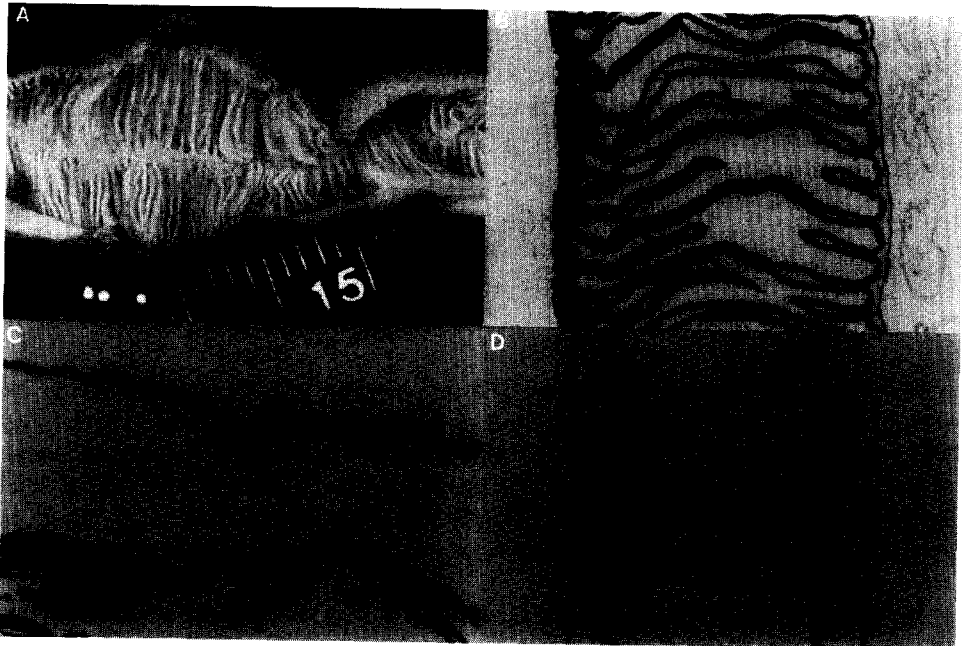


Fig. 3. (A) Photograph of dissected *Parastichopus* foregut showing numerous lamellae. Smallest ruler division equals 1 mm. (B) Micrograph of longitudinal histological section from the foregut showing surface-area enhancement by hollow lamellae. (C) Micrograph of longitudinal histological section from midgut region. (D) Micrograph of longitudinal histological section from hindgut region. Magnifications of B, C, and D are $2.5 \times$ those of A, so that one ruler unit $400 \mu\text{m}$.

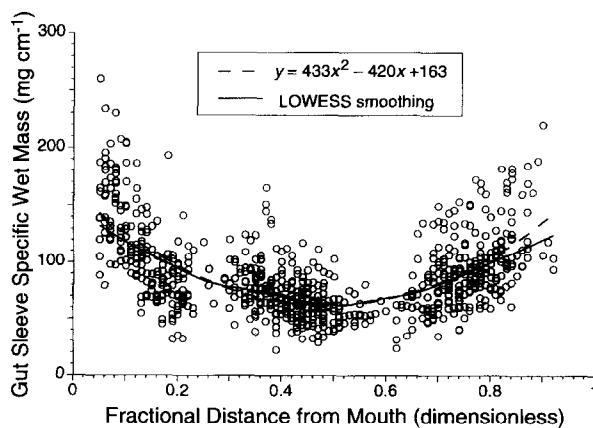


Fig. 4. Distribution of length-specific tissue mass along the gut of *Parastichopus*. Curves are LOWESS (Cleveland, 1979) smoothings and quadratic least-squares fits for 716 data points. For the regression, independence of sections taken from the same individual is assumed.

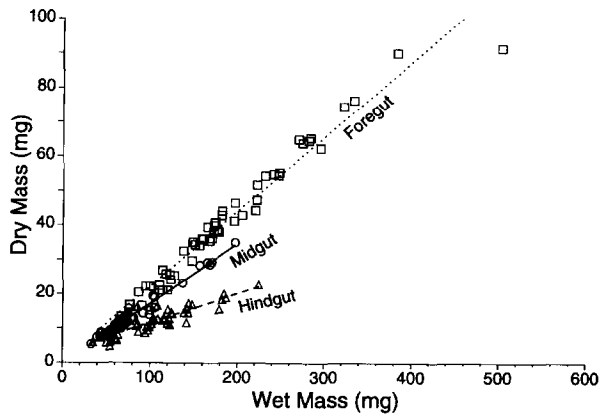


Fig. 5. Fore-, mid-, and hindgut sleeve dry mass versus wet mass. Lines are results of least-squares linear regressions treating each sleeve as independent.

should interact similarly with the lipid bilayers of cell membranes. The AA: L-glucose permeability ratio (Eq. 1) corrects for differences with the AA. All test substrates differ from L-glucose, however, in concentration gradient across the gut wall—which is proportional to diffusive flux. It is unlikely that L-glucose occurs in appreciable concentrations in cells, but D-glucose and AA are common ingredients. Therefore the D-glucose and AA concentration gradients should be less steep than that of L-glucose and thus L-glucose diffusive flux would be an overestimate of test substrate diffusive fluxes. Carrier-mediated fluxes were estimated as total flux minus diffusive L-glucose flux. Since the L-glucose flux is an overestimate, substrate carrier-mediated fluxes are underestimates. Comparing fluxes of D- and L-glucose at incubation solution concentrations much greater than K_m in mixtures with an adherent marker like PEG, would immediately saturate the D-glucose carrier and theoretically only D-glucose diffusive flux would be measured for comparison with L-glucose diffusive flux. Over the 6-min minimal incubation time required for PEG concentration to equilibrate between gut surface and bulk solution, however, both L- and D-glucose concentration gradients would decrease to zero and the effect of intracellular D-glucose concentration would be lost.

With these caveats in mind, we pooled measurements of D-glucose uptake rate from all gut sections of five *Parastichopus* individuals. The results strongly imply saturating, hyperbolic kinetics (Fig. 6). Fitting the data with a Michaelis-Menten equation by the medians method of nonlinear regression (Duggleby, 1981) we get $J_{max} = 26 \text{ pmol (mg tissue wet mass)}^{-1} \text{ min}^{-1}$ and $K_m = 122 \text{ } \mu\text{M}$ (Table 2), which significantly ($p = 0.03$) increased explained sum of squared deviations over the linear competitor (Table 3). The diffusive flux component, measured independently using radioactively tagged L-glucose paired with PEG, is linear within the experiment's concentration range, with a slope of $0.013 \text{ } \mu\text{l (mg tissue wet mass)}^{-1}$

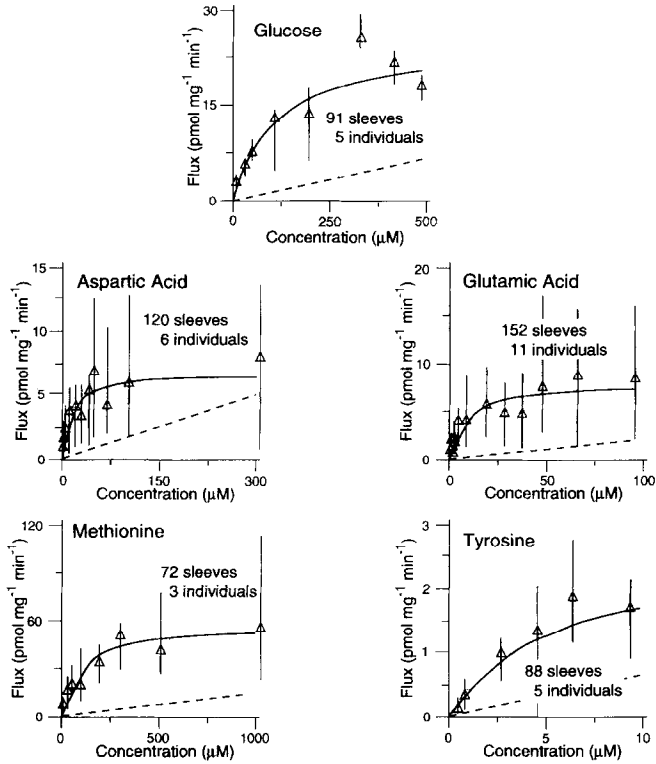


Fig. 6. Carrier-mediated (solid curve) and diffusive (dashed line) fluxes of substrates across the gut wall of *Parastichopus californicus*. Results from 2 to 4-min incubations (Table 1) followed by a 20-s rinse of fore-, mid- and hindgut sleeves. Median fluxes and concentrations (Δ), nonparametric 95% confidence intervals, linear (diffusive) and nonlinear (carrier-mediated) regressions (Duggleby, 1981) are plotted.

min⁻¹ (Fig. 6 and Table 2). The functional dependence of total glucose uptake rate (J_T) on luminal glucose concentration (C) is described as the sum of the carrier-mediated and passive components:

$$J_T = \frac{26 \cdot C}{122 + C} + 0.013 \cdot C. \quad (3)$$

Simple diffusion contributes substantially to total glucose uptake. For the concentration at which carrier-mediated uptake is half saturated (122 μM) passive uptake contributes ≈11% to total uptake (Table 2) versus less than 1% for mice (Karasov & Diamond, 1983).

Michaelis-Menten kinetics also apply to the four AA tested (Fig. 6). The nonlinear fits increased the explained component of the sum of squared deviations (Table 3), supporting the notion that a carrier-mediated AA uptake system operates in the *Parastichopus* gut. The contribution of diffusion to total uptake rate was small for aspartic acid, glutamic acid and methionine but increased to

Table 3

ANOVA results for multiple regression of carrier-mediated substrate flux J ($\text{pmol} \cdot \text{mg}^{-1} \cdot \text{min}^{-1}$) against substrate concentration, C (μM)

Source of variation	Sum of squares	df	Mean square	F	p
GLUCOSE					
Constant = median [$J = k_1$]	25732.7	1	25732.7	127	$\ll 0.001$
Regression model					
extra for linear model [$J = m \cdot C + k_2$]	4812.3	1	4812.3	24	$\ll 0.001$
extra for nonlinear model [$J = \frac{V_{max} \cdot C}{K_m + C}$]	1020.6	1	1020.6	5.0	0.03
Residuals	17496.0	88			
lack of fit	662.2	5	132.4	<1	NS
experimental error	16833.8	83	202.8		
Total	49061.6	91			
ASPARTIC ACID					
Constant = median [$J = k_1$]	2641.7	1	2641.7	105	$\ll 0.001$
Regression model					
extra for linear model [$J = m \cdot C + k_2$]	649.7	1	649.7	26	$\ll 0.001$
extra for nonlinear model [$J = \frac{V_{max} \cdot C}{K_m + C}$]	136.5	1	136.5	5.4	0.02
Residuals	2891.8	117			
lack of fit	147.1	8	18.4	<1	NS
experimental error	2744.7	109	25.2		
Total	6319.7	120			
GLUTAMIC ACID					
Constant = medium [$J = k_1$]	4132.6	1	4132.6	151	$\ll 0.001$
Regression model					
extra for linear model [$J = m \cdot C + k_2$]	1539.0	1	1539.0	56	$\ll 0.001$
extra for nonlinear model [$J = \frac{V_{max} \cdot C}{K_m + C}$]	158.7	1	158.7	5.8	0.02
Residuals	3943.0	149			
lack of fit	158.1	11	14.4	<1	NS
experimental error	3784.9	138	27.4		
Total	9773.3	152			

Table 3 (continued)

Source of variation	Sum of squares	df	Mean square	F	p
METHIONINE					
Constant = median [$J = k_1$]	69206.9	1	69206.9	119	≤0.001
Regression model					
extra for linear model [$J = m \cdot C + k_2$]	7241.0	1	7241.0	12	0.001
extra for nonlinear model [$J = \frac{V_{max} \cdot C}{K_m + C}$]	13694.3	1	13694.3	24	≤0.001
Residuals	36386.1	69			
lack of fit	< 0	5	< 0	≤1	NS
experimental error	37235.8	64	581.8		
Total	126528.3	72			
TYROSINE					
Constant = median [$J = k_1$]	75.8	1	75.8	126	≤0.001
Regression model					
extra for linear model [$J = m \cdot C + k_2$]	33.4	1	33.4	56	≤0.001
extra for nonlinear model [$J = \frac{V_{max} \cdot C}{K_m + C}$]	2.3	1	2.3	3.8	0.06
Residuals	50.9	85			
lack of fit	1.4	3	0.5	<1	NS
experimental error	49.5	82	0.6		
Total	162.4	88			

NS = not significant.

21% for L-tyrosine (Table 2). Chemical interaction between substrate and cell membrane explains these differences. The solubilities of methionine and tyrosine in water (Table 1) are inversely correlated with their passive permeability across the gut wall (Table 2). Molecular weight and solubility in oil (or conversely insolubility in water) are the major determinants of passive diffusion across cell membranes (Diamond & Wright, 1969). The molecular weights of methionine and tyrosine are similar, suggesting that interaction with the hydrophobic lipid bilayer of the cell membrane explains the difference in gut wall permeability. Tyrosine (with an aromatic ring) is more hydrophobic than methionine and thus diffuses across the cell membrane more easily. Aspartic and glutamic acids have intermediate solubilities in water (Table 1) –thus intermediate hydrophobicities and therefore permeabilities (Table 2).

AA J_{max} and K_m values also vary, suggesting unequal allotment and affinity of AA-specific carriers (Table 2). Numbers of aspartic and glutamic carriers are

nearly equal. Methionine appears to have the highest and tyrosine the lowest number of transporters. Perhaps methionine is hyperessential, requiring allocation of an unusual number of carriers to meet demand. Methionine has been found to be a precursor of taurine in the deposit-feeder *Arenicola cristata* (Abbott & Awapara, 1960) and in the suspension feeder *Mytilus edulis* (Awapara, 1962). Along with glycine (Giordano et al., 1950; Henrichs, 1980), taurine is often the dominant free AA in marine invertebrates, these AA functioning as osmoregulators or methyl group acceptors (Awapara, 1962). Transporter allotment among the AA substrates may also be influenced by supply in sedimentary food, digestive kinetics, demands of tissue synthesis, and physical-chemical constraints on passive uptake due to substrate interaction with the hydrophobic cell membrane. Methionine available to enzymatic digestion becomes increasingly scarce as detritus decays (Mayer et al., 1995), so there may be an especial premium on its acquisition where and while it is available.

AA compositions of food and tissue are end members of the digestion-absorption-synthesis chain. AA makeup of *Parastichopus* tissue (dominated by the body wall) is nearly identical to the microbe-covered sediment that it ingests (Table 4). In fact, compositional equality of AA among trophic groups (Vonk & Western, 1984, their Fig. 2.2) precludes their use as biomarkers (Cowie, 1990; Hedges & Prahl, 1993; Wakeham et al., 1993). There are some broad patterns, however. Diatoms are high in aspartic and (often) glutamic acids but low in methionine and tyrosine (Hecky et al., 1973). Bacterial S-layers, which may dominate the enzymatically hydrolyzable protein fraction in sediments (Mayer et al., 1995), are methionine deficient (Beveridge & Graham, 1991). Nonspecific enzymatic digestion produces AA concentrations in the gut lumen, reflecting relative abundance in food. Thus aspartic and glutamic concentration gradients across the gut wall will be greater than those of methionine and tyrosine. The higher aspartic and glutamic gradients offset their intermediate passive permeability (Table 2). Gradient-driven diffusion supplies ample monomer, requiring only moderate carrier-mediated uptake to meet synthetic demand. To offset

Table 4

Amino acid test substrate composition of *Parastichopus* tissue (including body wall, gut and respiratory tree), sediment food and gut fluid. Estimated total amino acid absorbed by carrier-mediated and passive uptake integrated over the total gut length

Substrate	Tissue composition (mole%) ^a	Sediment food composition (mole%) ^a	Gut fluid concentration (μM)			Total absorbed ^b
			Foregut	Midgut	Hindgut	
D-glucose	–	–	300	140	70	1.52
L-aspartic acid	10	11	10	11	5	0.17
L-glutamic acid	14	16	26	19	13	0.23
L-methionine	1	2	4	8	0.3	0.27
L-tyrosine	2	1	10	11	0.3	0.06

^a Mayer et al., 1995.

^b Integrated area under curves of Fig. 8; units are flux ($\text{nM} \cdot \text{cm}^{-1} \cdot \text{min}^{-1}$).

intermediate permeability and rarity in the sediment food, many methionine transporters are provided and reflected in the $8 \times$ greater J_{max} for methionine than for other AA. Tyrosine is also rare, but the weak concentration gradient between gut lumen and intracellular spaces is offset by the $4 \times$ higher permeability coefficient; thus, minimal carrier number is required.

3.3. Methionine: a hyperessential nutrient?

Some AA may be required for transient metabolic processes as well as synthesis. Higher relative demand is suggested by high ($>2 \times$) uptake capacity (J_{max}) relative to dietary intake (Diamond & Hammond, 1992) or tissue composition. These hyperessential nutrients, for which amount absorbed surpasses synthetic demand, could theoretically be identified by a disproportionately high amount absorbed relative to tissue composition.

Amounts of nutrients absorbed by the gut are determined during steady intake by uptake rates acting at steady luminal concentrations (of the products of digestion). On the assumption that gut passage time is the same for all AA and regional gut lumen concentrations are as measured (Table 4), we interpolated total flux (from total flux per unit of gut length vs. concentration curves, Fig. 7) at known gut sleeve locations. Smoothing of the raw data (Fig. 8) suggested that AA absorption peaked in the midgut. While absorption of acidic AA continued at high levels in the hindgut, methionine and tyrosine rates were very low there, due to low luminal concentrations of these more quickly released and rarer AA. Glucose rates were monotonically decreasing rearward. Integrating the areas under the curves estimated the total amount of glucose or AA absorbed (Table 4). Except for methionine, the pattern of rare and common AA in food and tissue extended to total absorbed. After rescaling (divide by the highest value in table columns) tissue and food composition, total absorbed (Table 4), AA passive permeability,

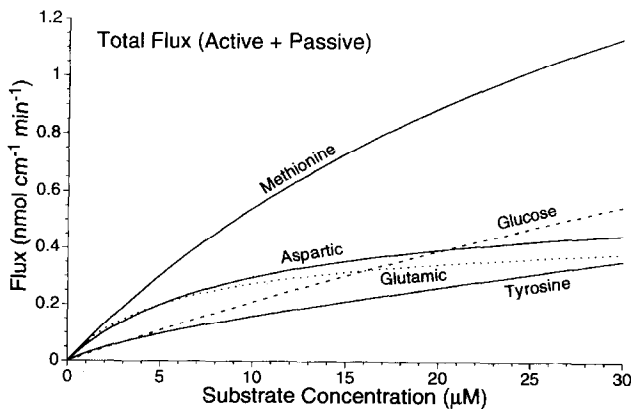


Fig. 7. Total (carrier-mediated + diffusive) AA and glucose flux across the gut wall.

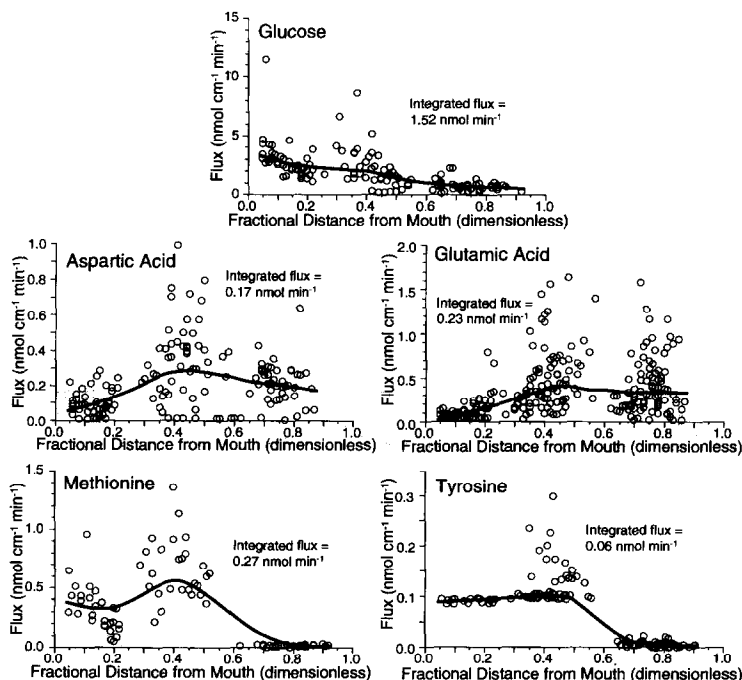


Fig. 8. Axial distribution of total glucose and AA uptake rates. Curves are LOWESS smoothings of rates interpolated from substrate flux-vs.-concentration data collected for Fig. 6 and experimentally measured fore-, mid-, and hindgut substrate luminal concentrations (Table 4). Points for tyrosine are “jittered” (SYSTAT) to reduce their overlap.

and J_{max} (Table 2) to facilitate comparison across substrates, methionine stood out with much more monomer absorbed than could be accounted for by tissue requirements (Fig. 9) and thus may be a hyperessential nutrient.

Our results suggest an experimental framework for isolating organic compounds essential to benthic deposit-feeders. The apparent balance between rates and end-member structural protein composition for three of four AA suggests that this pattern is the null hypothesis against which alternatives can be tested in future experiments. Divergence from this pattern by methionine (and literature citations suggesting additional physiological roles for methionine in benthic deposit feeders) reinforces this approach.

Lastly, our data allowed us to estimate the longitudinal distribution of carriers. Dade et al. (1990) posed the question of how absorptive sites should be distributed to achieve maximal absorption rate for a fixed number of absorbers. There can be no general answer because digestive production rates and therefore luminal concentration patterns in the absence of absorption vary. Further, large deposit feeders may suffer severe competition for digestive products from luminal

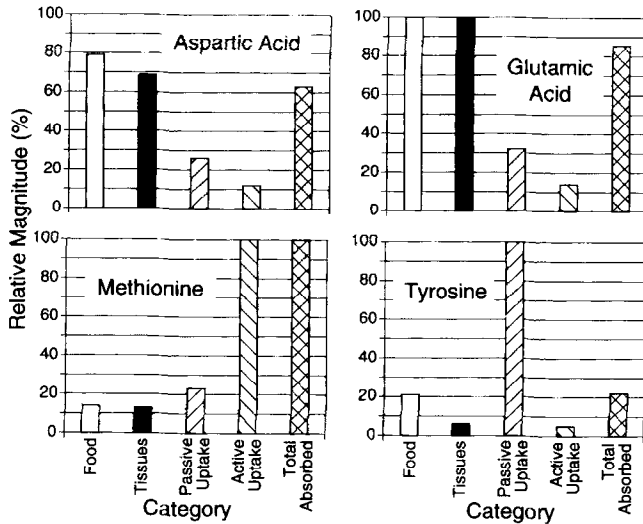


Fig. 9. Relative composition of AA in sediment food and animal tissue. Relative magnitude of permeability coefficients, J_{max} and total nutrient absorbed by the gut. All values are scaled across amino acids and glucose relative to the largest value in any one category: Glutamic acid showed highest food and tissue percentages, tyrosine showed the greatest passive uptake rate, and methionine showed the highest active uptake and integrated absorption rates.

bacteria (Plante et al., 1989, 1990), further changing the ideal distribution. Nonetheless it is of interest to ask whether any regular patterns emerge.

In order to estimate the local number of absorbers, we assumed that the nature of the carriers was invariant along the gut, i.e. that K_m was constant and that uptake rate at a given concentration in our everted-sleeve experiments therefore varied only with the number of carriers. In effect, we assumed a local V_{max} set by local carrier abundance. We drew a Michaelis-Menten plot with the fixed K_m through the observed “point” of uptake rate measured and concentration set in the sleeve experiments. Because these parameters are not the same as they are when expressed per unit of mass of tissue (Table 2), we recalculated them per unit of length (Table 5). We extrapolated this curve to the concentration (C_{99}) at which the rate of reaction would reach 99% of its maximal value to obtain an “apparent V_{max} ”. Under these assumptions, variations in the rate along the gut should be proportional to the number of carriers (Fig. 10).

Assuming that the cost to synthesize and maintain a carrier is roughly constant and independent of location, a reasonable null hypothesis is that carriers should be distributed so that the flux (gain) per carrier is roughly constant. Otherwise, it would be profitable to make additional carriers in the regions where additional flux could be achieved, at least until the added gain per carrier fell below the added cost per carrier. This expectation is met for glucose, aspartic acid and glutamic acid, which show remarkable similarity between Figs. 8 and 10. They

Table 5
Michaelis-Menten parameters expressed per unit of length of the gut

Substrate	J_{max} ($\text{nmol} \cdot \text{cm}^{-1} \cdot \text{min}^{-1}$)	K_m (μM)	C_{99} (mM)
D-glucose	2.6	119.6	10.2
L-aspartic acid	0.54	8.9	0.88
L-glutamic acid	0.4	5.4	0.53
L-methionine	2.37	35	3.47
L-tyrosine	0.10	4.6	0.46

C_{99} is the back-calculated concentration at which the flux would equal $0.99 J_{max}$. Specifically,

$$C_{99} = \frac{0.99 J_{max} K_m}{J_{max} - 0.99 J_{max}}$$

paint the typical physiological picture (Diamond & Hammond, 1992) of operation near K_m (or $V = V_{max}/2$). Methionine, on the other hand, shows further evidence of being hyperessential. Carriers are maintained in the hindgut despite the fact

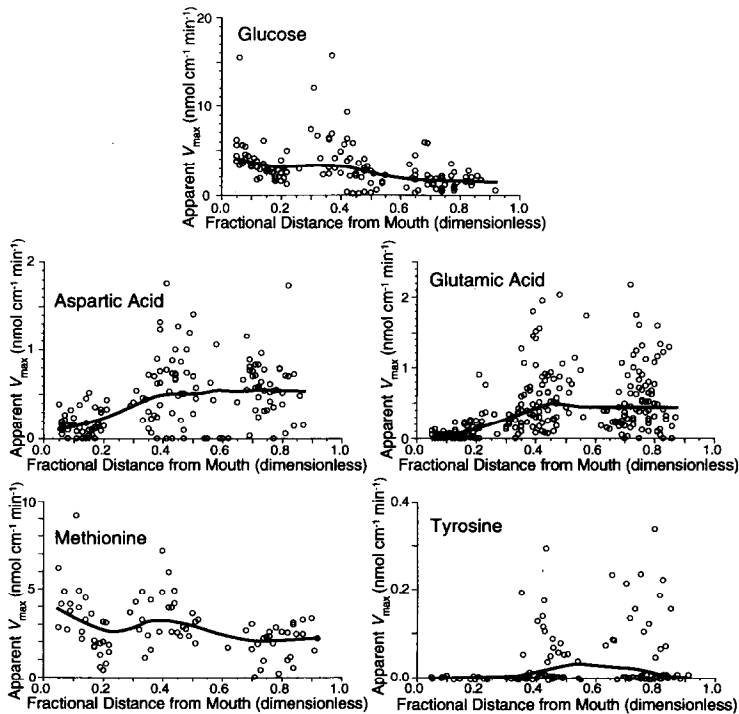


Fig. 10. Axial distribution of apparent V_{max} for absorption. Its values should be proportional to local carrier abundance (cm^{-1}). Curves are LOWESS smoothings of rates extrapolated from substrate flux-vs.-concentration data collected for Fig. 6. Points for tyrosine are “jittered” (SYSTAT) to reduce their overlap.

that in our measurements of luminal concentrations (Table 3) would not generate uptake there (Fig. 8). Apparently, occasional windfalls occur, with foods higher in methionine or slower in its release warranting maintenance of carriers in the hindgut. Furthermore, the ratio of capacity (Fig. 10) to observed flux (Fig. 8) is by far highest for methionine, supporting the impression of a hyperessential nutrient—with carriers poised to take in any available substrate. The picture for tyrosine is less clear. The scattering of high V_{max} values in the hindgut suggests, however, that for this scarce substrate carriers also extend rearward beyond the region where significant uptake normally is seen.

3.4. Gut throughput time, diet and future prospects

Gut throughput time decreased during spring from a late-winter value near 9 h to a plateau near 5 h and was relatively insensitive to gut length (Fig. 11). The

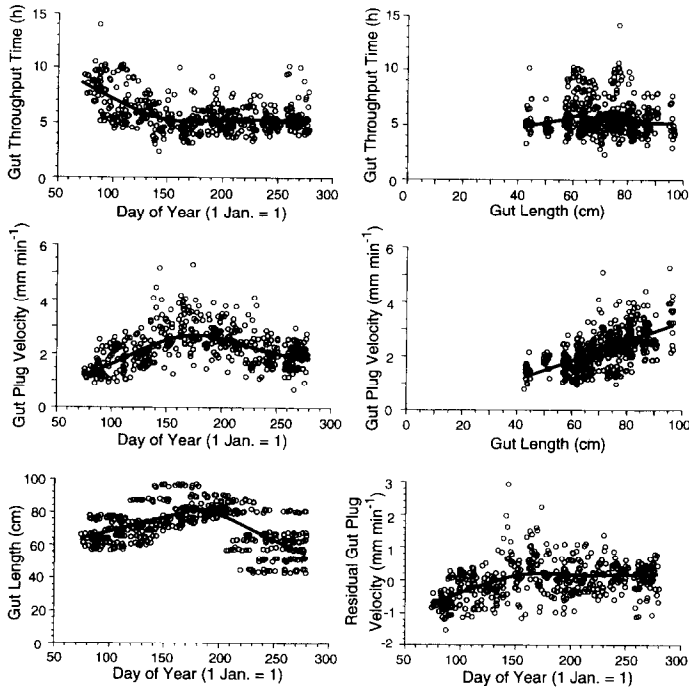


Fig. 11. Seasonal variation in gut throughput time and related variables in captive *Parastichopus californicus*. Residual gut plug velocity is the residual from the linear fit of gut plug velocity against gut length. Thick lines are LOWESS (Cleveland, 1979) smoothings of the 450 measurements or estimates except for the linear least-squares fit for gut plug velocity versus gut length. Only specimens larger than 40 cm gut length were collected. For about the first 70 and last 80 days of the year specimens with functional guts could not be obtained.

velocity of the plug through the gut, on the other hand, showed an apparent summer maximum, but this velocity was linearly related to gut length (Fig. 11). The apparent discrepancy between gut throughput time and plug velocity is reconciled by noting that gut length begins to decrease in late July or early August; when corrected for variation due to gut length, plug velocity mirrors throughput time (Fig. 11). Decrease in gut length is an indication of onset of seasonal atrophy in *Parastichopus californicus* (Fankboner & Cameron, 1985). We suspect that gut throughput time is regulated by the animal to correspond with the time needed to digest and absorb nutrients and that the short summer throughput times correspond with food of high lability. We also suspect that gut throughput time is cued by chemical stimuli in the food provided rather than being set by light or chemical cues in the open seawater supply because we see dramatic responses to altered food quality in some experimental treatments (Self & Jumars, unpubl. results).

Parastichopus californicus' high summer feeding rates followed by gut atrophy or evisceration provide further clues to diet. Populations in the Pacific Northwest (Swan, 1961; Fankboner & Cameron, 1985; Cameron & Fankboner, 1989), as well as their congeners in northern California (Yingst, 1982), Norway (Jespersen & Lützen, 1971) and Japan (Tanaka, 1958), lose their guts in the fall and regain them by the next spring. These results suggest that *Parastichopus californicus* is a dietary specialist on fresh phytoplankton detritus or fresh microphytobenthos, produced primarily from spring to fall, and may not be able to profit from poorer substrates. Supporting this conclusion further is its high ratio in activity of glucosidase versus other enzymes (Mayer et al., 1995), in accord with patterns found in other shallow-water holothuroids (Féral, 1989). Mobile surface deposit-feeding holothuroids like *Parastichopus californicus* are likely to be patch specialists on microalgae and fresh microalgal detritus. We note in particular from summer cores retrieved from the depths that *Parastichopus californicus* inhabits an abundant population of benthic diatoms that retain a daily migration pattern (downward at night) in the laboratory (Jumars & Self, unpubl.). Our observations underscore the large energetic expense of maintaining a gut, which must be greater when integrated over late fall and winter than the cost of replacing it entirely.

We have found *Parastichopus californicus* to be an excellent subject for study of absorptive uptake for several reasons. One is the fundamentally simple anatomy of digestion in echinoderms (De Ridder & Jangoux, 1982; Féral & Massin, 1982) coupled with long guts (up to 90 cm), allowing large sample sizes that facilitate detection of weak patterns. A second is the ability to induce evisceration. Because this induction is not necessarily fatal, it holds the prospect of future experiments in which an animal is conditioned to one food supply with particular AA ratios, is made to eviscerate, and then is conditioned to another food supply. Without this capability for nonfatal application of the Karasov & Diamond (1983) technique, paired statistical design (conditioning of the same individual to two or more different foods, with complete turnover of absorptive tissues) would be im-

possible. The paired design has the potential to remove much of the between-individual, genetic component of variance.

Karasov (1988) scored 42 vertebrate species on their ratio of glucose uptake to proline uptake and found average ratios near 2, 0.8 and 0.3 for herbivores, omnivores and carnivores, respectively. No matter which of the four amino acids tested here is chosen to produce such a ratio, *Parastichopus californicus* falls well above unity, suggesting herbivore status. We are not proposing that all deposit feeders will appear to be similar in this regard. In particular, no subsurface deposit feeders from deep water appear among the animals for which diet source can be inferred with confidence. There is also evidence from bulk C:N ratios of apparently assimilated material that even some intertidal surface deposit feeders may be dietary specialists on nitrogenous compounds in preference to sugars (Carey & Mayer, 1990), though this conclusion must be tempered because pre-ingestive selection was unquantified in this study.

Our study of a single species gives us no basis to infer that most deposit feeders will be found to assimilate digestive products in ratios similar to those of vertebrate herbivores or of *Parastichopus californicus*. We conclude rather that the Karasov & Diamond (1983) everted-sleeve technique has sufficient promise based on our results with one species and a few substrates to merit exploration with other substrates, other marine deposit feeders and marine representatives of other trophic groups. Now that active uptake has been established for a diversity of AA, experiments with selected oligopeptides can be considered in *Parastichopus*. Until a strategy for unraveling the vast combinatorial possibilities for oligomer uptake becomes clear, however, extreme results with monomers-like those we obtained for methionine-will continue to be most informative.

Acknowledgements

B. Karasov helped us get started with the everted-sleeve method. We thank the Director of Friday Harbor Laboratories for the use of facilities and resources. D. Duggins, J. Eckman and M. Woodbury collected animals for us. S. Sampson, Darling Marine Center, University of Maine, made the histological sections and determined gut surface areas. We also thank L. Schick for AA analysis. Art Woods, L. Karp-Boss and an anonymous reviewer made helpful suggestions for revision. Research and publication were supported by NSF grant OCE 92-02855.

References

- Abbott, W. & J. Awapara, 1960. Sulfur metabolism in the lugworm *Arenicola cristata* Stimpson. *Biol. Bull.*, Vol. 119, pp. 357–370.
- Ahearn, G.A., 1988. Nutrient transport by the invertebrate gut. In, *Advances in comparative and environmental physiology*, Vol. 2, edited by R. Jiles. Springer-Verlag, Berlin, pp. 91–129.

- Alpers, D.H., 1987. Digestion and absorption of carbohydrates and proteins. In, *Physiology of the gastrointestinal tract.*, second edition, edited by L.R. Johnson, Raven Press, New York, pp. 1469–1487.
- Awapara, J., 1962. Free amino acids in invertebrates: A comparative study of their distribution and metabolism. In, *Amino acid pools*, edited by T. Holden, Elsevier, New York, pp. 158–175.
- Bamford, D.R. & D. James, 1972. An in vitro study of amino acid and sugar absorption in the gut of *Echinus esculentus*. *Comp. Biochem. Physiol.*, Vol. 42A, pp. 579–590.
- Bamford, D.R. & M. Stewart, 1973a. Absorption of neutral amino acids by the gut of *Arenicola marina*. *J. Comp. Physiol.*, Vol. 82, pp. 291–304.
- Bamford, D.R. & M. Stewart, 1973b. Absorption of charged amino acids by the intestine of *Arenicola marina*. *Comp. Biochem. Physiol.*, Vol. 46A, pp. 537–547.
- Bamford, D.R., B. West & F. Jeal, 1972. An in vitro study of monosaccharide absorption in echinoid gut. *Comp. Biochem. Physiol.*, Vol. 42A, pp. 591–600.
- Beveridge, T.J. & L.L. Graham, 1991. Surface layers of bacteria. *Microbiol. Rev.*, Vol. 55, pp. 684–705.
- Bianchi, T.S. & J.S. Levinton, 1984. The importance of microalgae, bacteria and particulate organic matter in the somatic growth of *Hydrobia totteni*. *J. Mar. Res.*, Vol. 42, pp. 431–443.
- Box, G.E.P., W.G. Hunter & J.S. Hunter, 1978. *Statistics for experimenters*. John Wiley & Sons, New York, 653 pp.
- Cameron, J.L. & P.V. Fankboner, 1989. Reproductive biology of the commercial sea cucumber *Parastichopus californicus* (Stimpson) (Echinodermata:Holothuroidea). II. Observations on the ecology of development, recruitment, and the juvenile life stage. *J. Exp. Mar. Biol. Ecol.*, Vol. 127, pp. 43–67.
- Cammen, L.M., 1980. Ingestion rate: an empirical model for aquatic deposit feeders and detritivores. *Oecologia*, Vol. 44, pp. 303–310.
- Cammen, L.M., 1989. The relationships between ingestion rate of deposit feeders and sediment nutritional value. In, *Ecology of marine deposit feeders*, edited by G.R. Lopez, G.L. Taghon, and J.S. Levinton, Springer-Verlag, New York, pp. 201–222.
- Carey, D.A. & L.M. Mayer, 1990. Nutrient uptake by a deposit-feeding enteropneust: nitrogenous sources. *Mar. Ecol. Progr. Ser.*, Vol. 63, pp. 79–84.
- Cleveland, W.S., 1979. Robust locally weighted regression and smoothing scatter plots. *J. Am. Stat. Assoc.*, Vol. 74, pp. 829–836.
- Cowie, G.L., 1990. Marine organic diagenesis: A comparative study of amino acids, neutral sugars and lignin. Ph.D. Dissertation, University of Washington, Washington, 180 pp.
- Dade, W.B., P.A. Jumars & D.L. Penry, 1990. Supply-side optimization: maximizing absorptive rates. In, *Behavioural mechanisms of food selection, NATO ASI Series, Vol. G20*, edited by R.N. Hughes, Springer-Verlag, Berlin, pp. 531–556.
- De Ridder, C. & M. Jangoux, 1982. Digestive systems: Echinoidea. In, *Echinoderm nutrition*, edited by M. Jangoux & J.M. Lawrence, Balkema Press, Rotterdam, The Netherlands, pp. 213–234.
- Diamond, J.M. & K. Hammond, 1992. The matches, achieved by natural selection, between biological capacities and their natural loads. *Experientia*, Vol. 48, pp. 551–557.
- Diamond, J.M. & E.M. Wright, 1969. Biological membranes: The physical basis of ion and nonelectrolyte selectivity. *Annu. Rev. Physiol.*, Vol. 31, pp. 581–646.
- Duggleby, R.G., 1981. A nonlinear regression program for small computers. *Analyt. Biochem.*, Vol. 110, pp. 9–18.
- Fankboner, P.V. & J.L. Cameron, 1985. Seasonal atrophy of the visceral organs in a sea cucumber. *Can. J. Zool.*, Vol. 63, pp.2888–2892.
- Farmanfarmaian, A., 1969a. Intestinal absorption and transport in *Thyone*. I. Biological aspects. *Biol. Bull.*, Vol. 137, pp. 118–131.
- Farmanfarmaian, A., 1969b. Intestinal absorption and transport in *Thyone*. II. Observations on sugar transport. *Biol. Bull.*, Vol. 137, pp. 132–145.
- Farmanfarmaian, A., R. Socci & V. Iannaccone, 1982. Interactions of heavy metals with intestinal transport mechanisms. In, *Echinoderms: Proceedings of the International Conference, Tampa Bay*, edited by J.M. Lawrence, A.A. Balkema, Rotterdam, The Netherlands, pp. 339–344.

- Fenchel, T. & L.H. Kofoed, 1976. Evidence for exploitative interspecific competition in mud snails (Hydrobiidae). *Oikos*, Vol. 27, pp. 367–376.
- Féral, J.-P., 1989. Activity of the principal digestive enzymes in the detritivorous apodous holothuroid *Leptosynapta galliennei* and two other shallow-water holothuroids. *Mar. Biol.*, Vol. 101, pp. 367–379.
- Féral, J.-P. & C. Massin, 1982. Digestive systems: Holothuroidea. In: *Echinoderm nutrition*, edited by M. Jangoux & J.M. Lawrence, Balkema Press, Rotterdam, The Netherlands, pp. 191–212.
- Gardner, M.G., 1982. Absorption on intact peptides—studies on transport of protein digests and dipeptides across rat small intestines in vitro. *Q. J. Exp. Physiol.*, Vol. 67, pp. 629–637.
- Garnder, M.G., 1984. Intestinal assimilation of intact peptides and proteins from the diet—a neglected field? *Biol. Rev.*, Vol. 59, pp. 289–331.
- Giordano, M.F., H.A. Harper, & F.P. Filice, 1950. The amino acids of a starfish and a sea urchin (Asteroidea and Echinoidea). *Wasmann J. Biol.*, Vol. 8, pp. 129–132.
- Hecky, R.E., K. Mopper, P. Kilham & E.T. Degens, 1973. The amino acid and sugar composition of diatom cell-walls. *Mar. Biol.*, Vol. 19, pp. 323–331.
- Hedges, J.I. & F.G. Prahl, 1993. Early diagenesis: consequences for applications of molecular biomarkers. In: *Organic geochemistry*, edited by M. Engel & S.A. Macko, Plenum, New York, pp. 237–253.
- Henrichs, S.M., 1980. Biogeochemistry of dissolved free amino acids in marine sediments. Ph.D. Dissertation, Massachusetts Institute of Technology/Woods Hole Oceanographic Institution, Massachusetts.
- Hollander, M. & D.A. Wolfe, 1973. *Nonparametric statistical methods*. John Wiley & Sons, New York, New York, 503 pp.
- Horrocks, D.L., 1977. Error limits for dual label samples. *Technical information 1130 NUC-77-8T*. Beckman Scientific Instruments Division, Irvine, CA.
- Hummel, H., 1985. Food intake and growth in *Macoma balthica* (Mollusca) in the laboratory. *Neth. J. Sea Res.*, Vol. 19, pp. 77–83.
- Hyman, L.H., 1955. *The invertebrates: echinodermata*. McGraw-Hill, New York, 763 pp.
- Jespersen, Å. & J. Lützen, 1971. On the ecology of the aspidochirote sea cucumber *Stichopus tremulus* (Gunnerus). *Norw. J. Zool.*, Vol. 19, pp. 117–132.
- Jumars, P.A., 1993. Gourmands of mud: Diet selection in marine deposit feeders. In: *Diet selection*, edited by R.N. Hughes. Blackwell Scientific Publications, Oxford, pp. 124–156.
- Karasov, W.H., 1988. Nutrient transport across vertebrate intestines. In: *Advances in comparative and environmental physiology*, Vol. 2, edited by R. Jiles, Springer-Verlag, Berlin, pp. 131–172.
- Karasov, W.H. & J.M. Diamond, 1983. A simple method for measuring intestinal solute uptake in vitro. *J. Comp. Physiol.*, Vol. 152, pp. 105–116.
- Lawrence, D.C., A.L. Lawrence, M.L. Greer & D. Mailman, 1967. Intestinal absorption in the sea cucumber, *Stichopus parvimensis*. *Comp. Biochem. Physiol.*, Vol. 20, pp. 619–627.
- Li, Y. & S. Gregory, 1974. Diffusion of ions in sea water and in deep sediments. *Geochim. Cosmochim. Acta*, Vol. 38, pp. 703–714.
- Lopez, G., G. Taghon & J. Levinton, editors, 1989. *Ecology of marine deposit feeders*. Springer-Verlag, New York, 322 pp.
- Martinez del Rio, C. & W.H. Karasov, 1990. Digestion strategies in nectar-eating and fruit-eating birds and the sugar composition of plant rewards. *Am. Nat.*, Vol. 136, pp. 618–637.
- Matthews, D.M., 1975. Intestinal absorption of peptides. *Physiol. Rev.*, Vol. 55, 537–608.
- Matthews, D.M. & S.A. Adibi, 1976. Peptide absorption. *Gastroenterology*, Vol. 71, pp. 151–161.
- Mayer, L.M., L.L. Schick, T. Sawyer, C.J. Plante, P.A. Jumars & R.F.L. Self, 1995. Bioavailable amino acids in sediments: a biomimetic, kinetics-based approach. *Limnol. Oceanogr.*, Vol. 40, pp. 511–520.
- McMeekin, T.L., 1975. The solubility of biological compounds. In: *Solutions and solubilities*, Vol. VIII: *Techniques of Chemistry*, edited by M.R.J. Dack, Wiley, New York, pp. 443–465.
- Minami, H., E.L. Morse & S.A. Adibi, 1992. Characteristics and mechanisms of glutamine-dipeptide absorption in human intestines. *Gastroenterology*, Vol. 103, pp. 3–11.
- Newell, R.C., 1965. The role of detritus in the nutrition of two marine deposit feeders, the prosobranch *Hydrobia ulvae* and the bivalve *Macoma balthica*. *Proc. Zool Soc. Lond.*, Vol. 144, pp. 25–45.

- Parsons, T.R., Y. Maita & C.M. Lalli, 1984. *A manual of chemical and biological methods for seawater analysis*. Pergamon, New York, 173 pp.
- Payne, J.W., 1980. Energetics of peptide transport in bacteria. In, *Microorganisms and nitrogen sources*, edited by J.W. Payne, Wiley, New York, pp. 359–373.
- Penry, D.L., 1989. Tests of kinematic models for deposit-feeders' guts: patterns of sediment processing by *Parastichopus californicus* (Stimpson) (Holothuroidea) and *Amphitecis scaphobranchiata* Moore (Polychaeta). *J. Exp. Mar. Biol. Ecol.*, Vol. 128, pp. 127–146.
- Penry, D.L. & P.A. Jumars, 1987. Modeling animal guts as chemical reactors. *Am. Nat.*, Vol. 129, pp. 69–96.
- Plante, C.J., P.A. Jumars & J.A. Baross, 1989. Rapid bacterial growth in the hindgut of a marine deposit feeder. *Microbial Ecol.*, Vol. 18, pp. 29–44.
- Plante, C.J., 1990. Digestive associations between marine detritivores and bacteria *Annu. Rev. Ecol. Syst.*, Vol. 21, pp. 93–127.
- Plauth, M., I. Kremer, A. Raible, P. Stehle, P. Fürst & F. Hartman, 1992. Nitrogen absorption from isonitrogenous solutions of L-leucyl-L-leucine and L-leucine: a study in the isolated perfused rat small intestine. *Clin. Sci.*, Vol. 82, pp. 283–290.
- Prinslow, T.E., I. Valiella & J.M. Teal, 1974. The effect of detritus and ration size on the growth of *Fundulus heteroclitus* (L.). *J. Exp. Mar. Biol. Ecol.*, Vol. 16, pp. 1–10.
- Robertson, J.R. & S.Y. Newell, 1982. Experimental studies of particle ingestion by the sand fiddler crab *Uca pugilator* (Bosc). *J. Exp. Mar. Biol. Ecol.*, Vol. 59, pp. 1–21.
- Smith, G.N. & M.J. Greenberg, 1973. Chemical control of the evisceration process in *Thyone briareus*. *Biol. Bull.*, Vol. 144, pp. 421–436.
- Sober, H.A., editor, 1970. *CRC Handbook of biochemistry*. Chemical Rubber Company, Cleveland, OH, Table B-66.
- Stevens, B.R., H.J. Ross, & E.M. Wright, 1982. Multiple transport pathways for neutral amino acids in rabbit jejunal brush border vesicles. *J. Membr. Biol.*, Vol. 66, pp. 213–225.
- Stewart, M.G., 1981. Kinetics of dipeptide uptake by the mussel *Mytilus edulis*. *Comp. Biochem. Physiol.*, Vol. 69A, pp. 311–315.
- Stuart, V., E.J.H. Head & K.H. Mann, 1985. Seasonal changes in the digestive enzyme levels of the amphipod *Corophium volutator* (Pallas) in relation to diet. *J. Exp. Mar. Biol. Ecol.*, Vol. 88, pp. 243–256.
- Swan, E.F., 1961. Seasonal evisceration in the sea cucumber, *Parastichopus californicus* (Stimpson). *Science*, Vol. 133, pp. 1078–1079.
- Taghon, G.L., 1988. The benefits and costs of deposit feeding in the polychaete *Abarenicola pacifica*. *Limnol Oceanogr.*, Vol. 33, pp. 1166–1175.
- Taghon, G.L. & R.R. Greene, 1990. Effects of sediment-protein concentration on feeding and growth rates of *Abarenicola pacifica* Healy et Wells (Polychaeta: Arenicolidae). *J. Exp. Mar. Biol. Ecol.*, Vol. 136, pp. 197–216.
- Tanaka, Y., 1958. Feeding and digestive processes of *Stichopus japonicus*. *Bull. Fac. Fish. Hokkaido Univ.*, Vol. 9, pp. 14–28.
- Tate, M.W. & R.C. Clelland, 1957. *Nonparametric and shortcut statistics*. Interstate Publishers, Danville, Illinois, 171 pp.
- Tenore, K.R., R.B. Hanson, J. McClain, A.E. Maccubin & R.E. Hodson, 1984. Changes in composition and nutritional value to a benthic deposit feeder of decomposing detritus pools. *Bull. Mar. Sci.*, Vol. 35, pp. 299–311.
- Thamotharan, M. & G.A. Ahearn, 1995. Dipeptide transport by crustacean hepatopancreatic brush border membrane vesicles. *J. Exp. Mar. Biol. Ecol.* (submitted).
- Thwaites, D.T., B.H. Hirst & N.L. Simmons, 1993. Direct assessment of dipeptide/H⁺ symport in intact human intestinal (Caco-2) epithelium: a novel method utilising continuous intracellular pH measurement. *Biochem. Biophys. Res. Commun.*, Vol. 194, pp. 432–438.
- Vonk, H.J. & J.R.H. Western, 1984. *Comparative biochemistry and physiology of enzymatic digestion*. Academic Press, New York, New York, 501 pp.
- Wakeham, S.G., J.I. Hedges, C. Lee & T.K. Pease, 1993. Effects of poisons and preservatives on the composition of organic matter in a sediment trap experiment. *J. Mar. Res.*, Vol. 51, pp. 669–696.

- Weast, R.C., editor, 1979. *CRC Handbook of chemistry and physics*. CRC Press, Boca Raton, FL, Table F-62.
- Wilkinson, L., M. Hill & E. Vang, editors, 1992. SYSTAT. Graphics, SYSTAT, Inc., Evanston, Illinois, 600 pp.
- Windholz, M., editor, 1983. *Merck Index*. Merck and Co., Inc., Rahway, New Jersey, pp. 638–639.
- Wolfrath, B., 1992. Field experiments on feeding of European fiddler crab *Uca tangeri*. *Mar. Ecol. Progr. Ser.*, Vol. 90, pp. 39–43.
- Yingst, J.Y., 1982. Factors influencing rates of sediment ingestion by *Parastichopus parvimensis* (Clark), an epibenthic deposit-feeding holothurian. *Estuarine Coastal Shelf Sci.*, Vol. 14, pp. 119–134.